Philosophical Magazine Letters, Vol. 94, pp. 688-695 (2014).

Electropulsing-induced steels strengthening at high temperature

W.J. Lu*, X.F. Zhang and R.S. Qin*

Department of Materials, Imperial College London, Exhibition Road, London SW7 2AZ, United Kingdom.

Abstract

Electropulsing usually reduces the stability of metastable phases in materials. This work reports the opposite effect, where electropulsing drives the stable δ-phase at high temperature to be decomposed. This enables both γ-phase and σ-phase in duplex stainless steel to survive and hence to strengthen the steel at high temperature. The hardness of the quenched sample after electropulsing is 49.4% higher than that without electropulsing treatment. The scientific understanding to the observation has been developed.

Keywords: Electropulsing; phase stability; electrical properties; athermal effect; decomposition; strengthening

*Corresponding author. Tel.: +44 (0)20 7594 6803; fax: +44 (0)20 7594 6757; email: wenjun.lu09@imperial.ac.uk (W.J. Lu); r.qin@imperial.ac.uk (R.S. Qin)

1. Introduction

Steels become soft at high temperature. This is partly due to the dissolution of strong particles such as precipitates and phases. In principle, there are two physical methods to enable the strong particles to survive at high temperature. One is to introduce a mechanism to stabilize those particles directly. Another is to destabilize other associate phases in order to promote the reaction that causes the particles to appear.

Electropulsing usually reduces the stability of metastable structures. For example, the metastable $Fe_{78}B_{13}Si_9$ amorphous alloy loses its stability and crystalizes at 673 K (400 ^{o}C) under electropulsing, which would otherwise survive to 723 K (450 ^{o}C) in annealing [1]. Electropulsing induces the spheroidization of cementite at ambient temperature, which is much lower than that in annealing and without electropulsing [2]. The mechanisms behind these observations are the electropulsing-reduced kinetic barrier for structure transformation [3] and electropulsing-enhanced mobility for solutes and dislocations [4]. The temperature rising due to ohm heat, when it is significant due to the percolation effect of electric current, may also accelerate the transformation of metastable phases.

However, thermodynamic theory predicts that electropulsing may enhance the stability of the metastable phase if its electrical resistivity is lower than that of the stable phase [5-6]. This situation has rarely been seen in practise to the knowledge of the authors. The examples mentioned earlier in the present work are all in the opposite situation, e.g. a metal with the amorphous structure has higher electrical resistivity than that in crystal structure.

The electrical resistivity of pure iron drops when its crystal structure changes from the body-centred-cubic (δ-phase) to the face-centred-cubic (γ-phase) at 1667 K (1394 ^{o}C). The values obtained by experimental measurement are around $1.28\times10^{-6}\Omega\cdot$m for δ-phase and $1.26\times10^{-6}\Omega\cdot$m for γ-phase at a temperature around the transformation temperature respectively [7]. The resistivity-temperature coefficient for δ-phase is smaller than that for γ-phase. One can therefore reasonably suggest that the electrical resistivity of the δ-phase is extracted to be $1.30\times10^{-6}\,\Omega\cdot$m, which is higher than that of γ-phase ($1.05\times10^{-6}\,\Omega\cdot$m) at around 1108K (835 ^{o}C). Although the electrical resistivity of steels may have different behaviours from that of the pure iron, the structure-dependent and temperature-dependent trends of electrical resistivity should not be far away from that of pure iron because iron is anyway the dominant

element in steel. Once the electrical resistivity of γ-phase is lower than that of δ-phase in steels, electropulsing will be able to stabilize a fraction of γ-phase rather than that of δ-phase.

In the present work, a duplex stainless steel contains a phase transition that can be represented as $\delta \rightarrow \gamma + \sigma$ in a temperature up to 840°C. The equilibrium phase diagram of the steel has been calculated using MTDATA commercial code package with TCFE4 commercial database for steels, as demonstrated in Figure 1. According to the previous study, secondary γ-phase appears in the form of islands in a matrix of δ-phase, wrapped with σ-phase having a lacy morphology [8]. Both γ-phase and σ-phase are strong and usually in small particles that can strengthen steel, although the phase σ is not favourable from corrosion point of view.

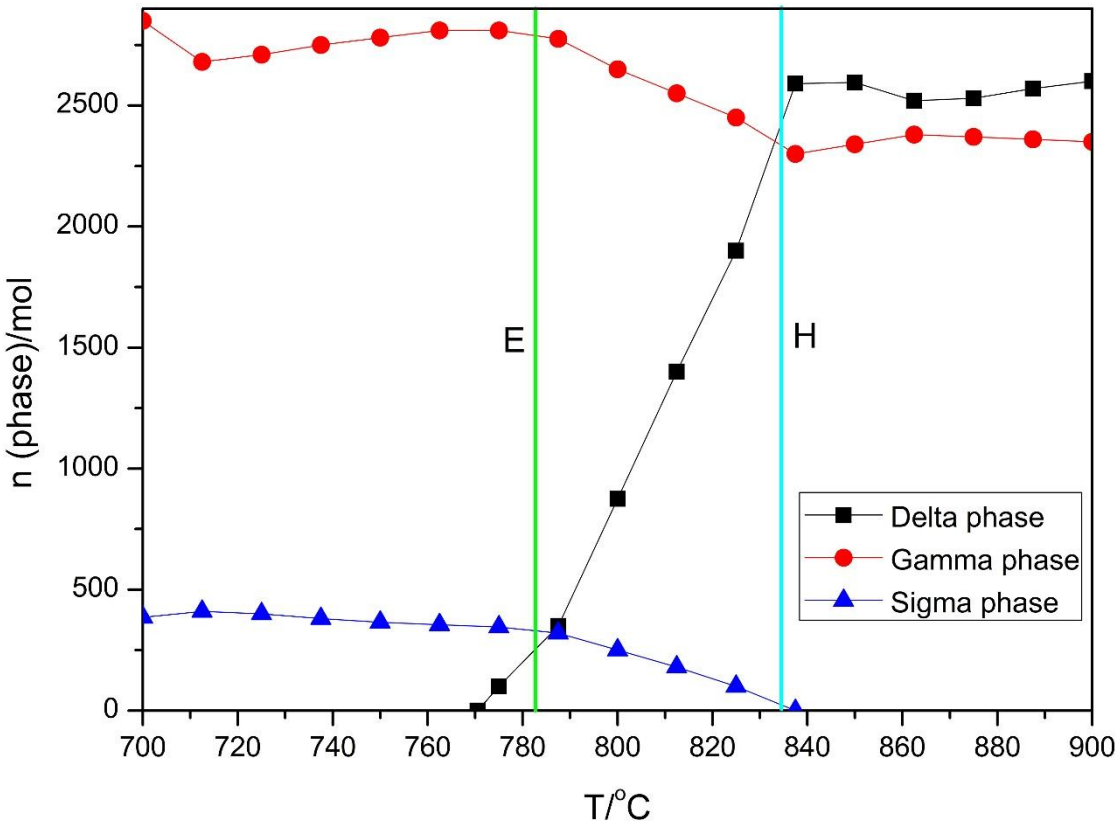

Figure 1 Equilibrium phase diagram of Fe-66.77, C-0.03, Mn-2.00, Si-1.00, S-0.015, P-0.035, Cr-22.00, Ni-5.00, Mo-3.00 and N-0.15 (wt.%) alloy calculated using MTDATA software with TCFE4 database. The total weight of the alloy is 100 kg. The value in bracket represents the weight of the element.

2. Experimental procedure

A commercial 2205 duplex stainless steel with chemical compositions (Fe-0.03C-2.00Mn-1.00Si-0.015S-0.035P-22.00Cr-5.00Ni-3.00Mo-0.15Nwt.%) was prepared, hot rolled to 3 mm thickness and then cold-rolled to 1.5 mm thickness before cut into many 1.5mm×2.0mm×15mm samples. A pair of samples were chosen randomly, put into the centre of a preheated furnace simultaneously and located next to each other for treatment. One of the samples was connected to an electropulse-generator using copper wires. Another sample was only annealed at the same thermal conditions as that connected to electropulsing but was not pulsed. The temperatures at both samples were measured using thermocouple and calibrated to ensure to be 835°C. The electropulsing parameters are: peak current density = 5×10^7 A/m^2, pulse duration = 60 μs, pulse frequency = 1 Hz. The annealing and electropulsing treatment lasted for 40 minutes before quenched in cold water. The electrical resistance of samples with and without electropulsing were measured by Microhmmeter (DO5000 series). The cooled specimens were mounted, polished and etched with a Marble reagent for metallographic examination using scanning electron microscopy (SEM) and hardness measurement using 2 kg load. After that, the samples were re-polished for X-ray diffraction (XRD) and electron backscattered diffraction (EBSD) analysis. The same procedures were repeated for 3 pairs of different samples. The similar results were obtained.

3. Results and discussion

The SEM image for the sample without electropulsing is presented in Figure 2a. The phases δ, γ and σ can be clearly seen and are labelled in the image. The SEM image for the sample with electropulsing is shown in Figure 2b. The microstructure demonstrated in Figure 2b is drastically different from that in Figure 2a. The effect of electropulsing on the amount of phases has been examined using XRD. Their spectrums are presented in Figure 3. In comparison of the patterns with and without electropulsing treatment, it is noticed that the amount of δ phase in (110), (200) and (211) orientation planes has been reduced significantly by electropulsing. The amount of γ-phase, as well as that of σ precipitate, has been increased. Quantitative calculation reveals the volume fractions of three phases in the sample without electropulsing are: 54% δ-phase, 44.8% γ-phase and 1.2% σ-phase. The values are in agreement with that predicted by CALPHAD at 835°C, as is labelled by the line H in Figure 1. The sample with electropulsing has the volume fractions of 5.2% δ-phase, 87.68% γ-phase and 7.12% σ-phase, respectively. This is similar to equilibrium volume fractions of the phases

at 780°C, as labelled by line E in Figure 1. Given the fact that the temperature in the sample is actually 835°C, it can be concluded that the electropulsing promoted the decomposition of $\delta \rightarrow \gamma + \sigma$ although this transition should be harder to occur at high temperature. Therefore, the austenite phase (the majority phase) is stabilized by electropulsing. This allows σ phase (the minority phase) particles to survive to higher temperature. Those two types of particles provide strengthening to the steel at high temperature.

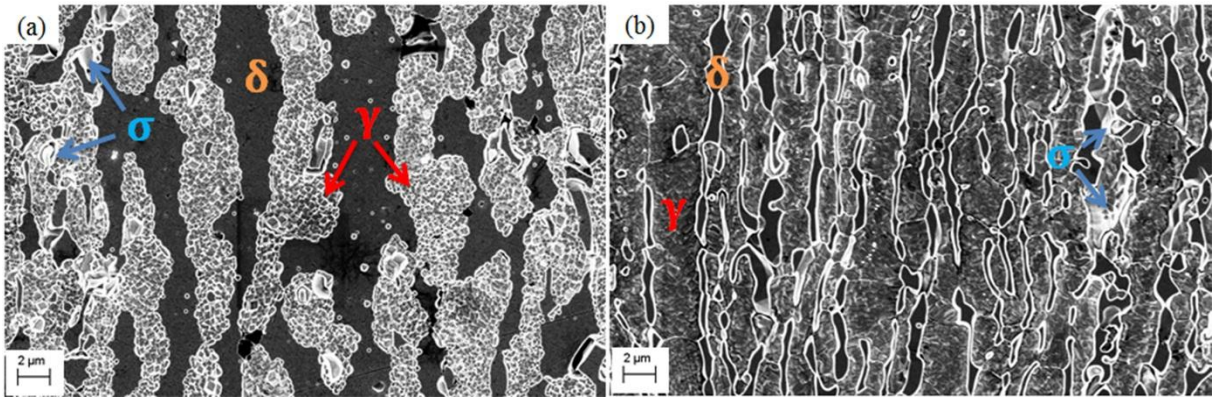

Figure 2 SEM images of the samples annealed (a) without and (b) with electropulsing at 835°C for 40 minutes.

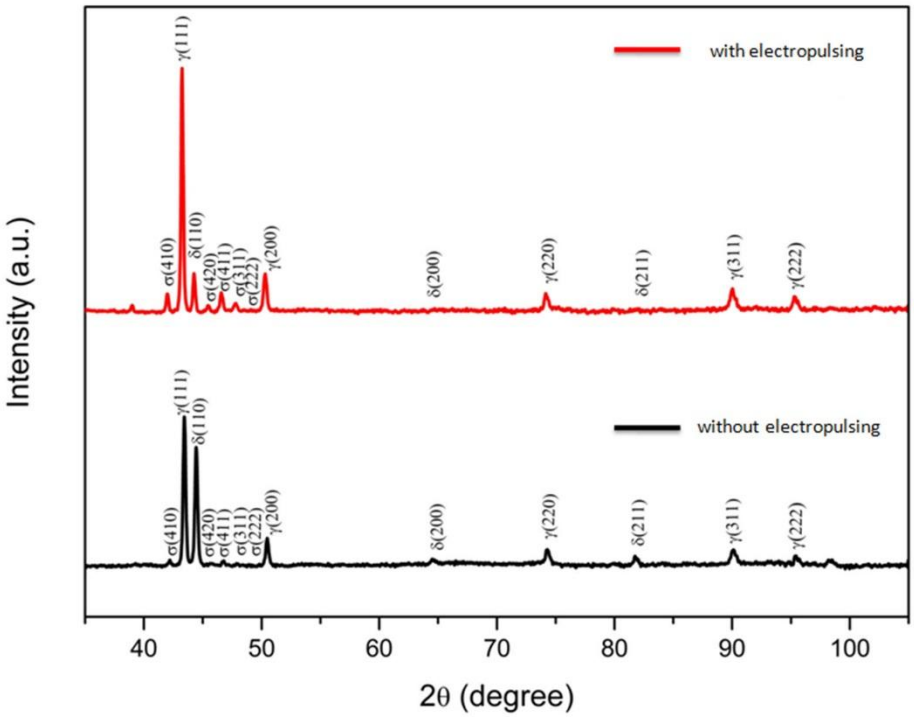

Figure 3 XRD spectrums for samples with and without electropulsing during annealing reveal the different fraction of δ, σ and γ phases.

The EBSD results provide clear information on the phase fraction in the samples. Figure 4a is the EBSD phase map for the sample without electropulsing and Figure 4b the map for the sample with electropulsing, where red represents the phase γ, green the phase δ, and white the phase σ. The image analysis provides the similar volume fraction of phases as that by XRD analysis. The results show clearly that electropulsing stabilizes γ-phase and σ-phase so that both phases have been retained at the temperature.

The EBSD orientation maps provide information for grains in the steel. Figure 4c and 4d illustrate the grain orientations in the samples without and with electropulsing treatment, respectively. Electropulsing induces the average grain size of γ-phase to reduce from 0.894 μm to 0.651 μm and that of δ-phase to reduce from 0.649 μm to 0.483 μm, respectively. The electropulsing-induced microstructure refinement in other alloys has been discussed

extensively in literatures [9]. The electropulsing-enhanced dislocation mobility in annealing of cold-worked samples is one of the major reasons.

Figure 4e and 4f present Σ3 grain boundary distribution map for the sample without and with electropulsing, respectively. Despite the grain refinement, EBSD analysis reveals that the electropulsing helps to increase the total fractions of Σ3 grain boundary from 22.6% to 27.5% throughout the sample. Σ3 grain boundary provides excellent corrosion resistance and is highly recommended in term of the grain boundary engineering [10]. On the other side, Σ3 grain boundary has lower electrical resistivity than that of normal grain boundary [11]. Electropulsing promotes the Σ3 grain boundary formation is within the thermodynamic prediction [12].

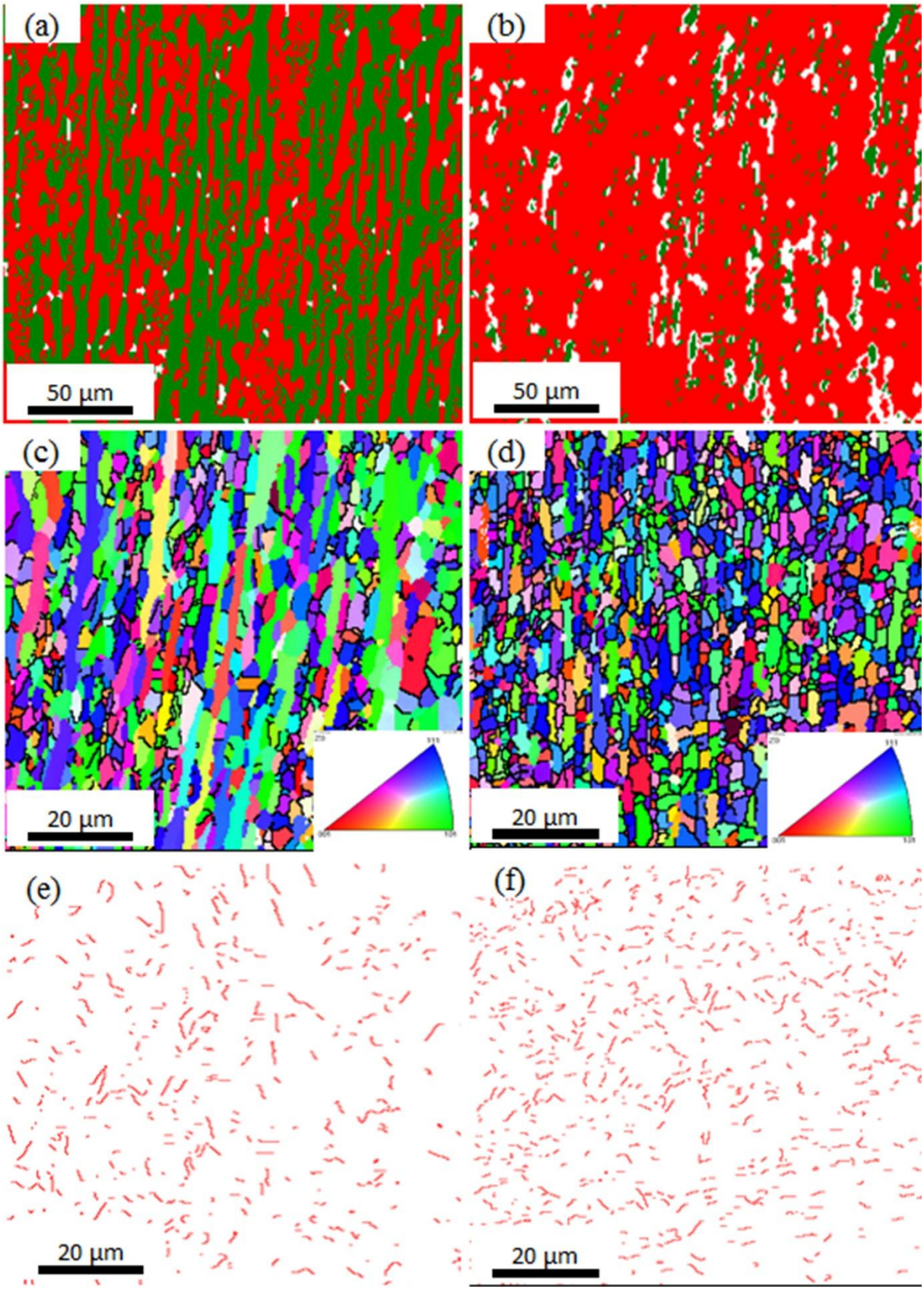
(a)
50 μm
(b)
50 μm
(c)
20 μm
(d)
20 μm
(e)
20 μm
(f)
20 μm

Figure 4 EBSD results demonstrate the fraction of phases (a) without electropulsing (b) with electropulsing, where the red region is γ, the green region corresponds to δ and the white region represents σ; the grain sizes and crystal orientations (c) without electropulsing and (d) with electropulsing; the Σ 3 grain boundary distribution (e) without electropulsing and (f) with electropulsing.

The Vickers hardnesses of the quenched sample without electropulsing is 316 HV and that with electropulsing treatment 472.4 HV, respectively. Electropulsing induced the increase of Vickers hardness by 49.4%. The tensile strength of the steel is proportional to the Vickers hardness. Therefore, one can estimate that the electropulsing may increase the tensile strength of the steel by roughly 49.4%. The increased strength is mainly due to the increasing amount of γ and σ phase particles that provide strengthening to the steel. Because the microstructure is the quenched from 835^{o}C, the strengthening mechanism is available for the steel at that temperature. Therefore, one can conclude that the strength of the steel at 835^{o}C should be increased by γ and σ phase particles that retained by electropulsing. The actual measurement of the strength at 835^{o}C should be carried out when facilities are available.

The electrical resistivity of sample without and with electropulsing are $7.19\times10^{-7}\Omega\cdot$m and $4.10\times10^{-7}\Omega\cdot$m, respectively. This is in good agreement with previous work for the effect of electropulsing on reducing electrical resistivity of steel [13]. The main hypothesis for the observed event may be developed from the fact that upon the onset of difference in Gibbs free energy of the system in duplex stainless steel at elevated temperature, via electropulsing. The phase equilibrium is calculated by minimizing the total free energy. The change of total free energy (ΔG_{tot}) in the steel with electropulsing is made up of two major parts, namely the change of the chemical free energy (ΔG_{chem}) and the change of the electropulsing free energy (ΔG_{elec}). This is expressed as following

$$\Delta G_{tot} = \Delta G_{chem} + \Delta G_{elec}. \quad (1)$$

The equilibrium phase diagram presented in Figure 1 is based on the minimization of chemical free energy only, which is suitable for the steel without electropulsing treatment. This has been confirmed by the fraction of phases in the sample annealed without electropulsing. Some γ-phases will be transformed into δ-phase when the temperature is

increased from 780°C to 835°C. However, the equilibrium phase diagram for the steel with electropulsing should be calculated by ΔG_{tot}, which requires the value of ΔG_{elec} [6]

$$\Delta G_{elec} = a\mu \frac{n-1}{n+2} j_o^2 V , \quad (2)$$

where a is a geometric factor, μ the magnetic permeability, j_0 is the average electric current density, V the volume of phase being transformed from original (electrical conductivity ρ_1) to new structure (electrical conductivity ρ_2), and $n = \rho_2 / \rho_1$. It can be seen that $\Delta G_{elec} < 0$ when $\rho_2 < \rho_1$. The retained extra γ-phase by electropulsing allows extra chemical free energy increases at equilibrium state ($\Delta G_{chem} = -\Delta G_{elec}$). The pattern in Figure 1 should therefore be shifted toward the right. This has been further proved by our experiment at 970°C, where the fraction of austenite is increased 5.6% by electropulsing in comparison to that without electropulsing treatment.

In general, the yield strength of alloys decreases with temperature as mentioned in *introduction* section. The decrease of tensile strength observed after annealing at temperatures from 800 to 1200°C in 2205 duplex stainless steel can be attributed to the increased δ-phase fraction [14]. However, in the present work, electropulsing provides an alternative method, which retarded the dissolution of γ and σ phase to higher temperature by δ-phase decomposition that benefited to enhance the strengthening effect. For this case, the alloy is said to exhibit yield strength anomaly, which is typical for superalloys and leads to their use in applications requiring high strength at high temperatures. Furthermore, the precipitation strengthening of alloy induced by precipitates and carbides is accompanied by sacrificing the corrosion resistance at high temperature in stainless steels and superalloys [15,16]. In order to enhance their resistance to oxidation and vulcanization at high temperature, a thermal barrier coating muse be added in the superalloys [17]. In the present work, electropulsing promoted the formation of Σ3 grain boundary that compensated the losses of corrosion resistance due to the formation of σ particles. Therefore the method provides a potential application for the steel as a superalloy candidate due to its improved strength and balanced corrosion-resistance.

4. Conclusion

In summary, electropulsing changes the equilibrium phase fraction in steels due to the differences of electrical resistivity of different phases. This allows to manipulate the

microstructure of steel and hence its mechanical properties. Electropulsing stabilises the γ-phase and σ-phase in duplex stainless steel and pushes the $\delta \rightarrow \gamma + \sigma$ transformation toward higher temperature than that without electropulsing. The survived σ-phase hard particles and γ-phase provide strengthening to the steel and made the steel strong at high temperature. Electropulsing also promotes the formation of Σ3 grain boundary, which can compensate the losses of corrosion resistance due to the formation of σ particles. When the microstructure is quenched to ambient temperature, the electropulsed sample has much higher hardness than that without electropulsing treatment.

Acknowledgment

The authors are grateful for financial support from EPSRC (EP/J011460/1), TATA Steel and the Royal Academy of Engineering toward the project.

References

[1] Z.H. Lai, H. Conrad, G.Q. Teng, Y.S. Chao, Mater. Sci. Eng. A 287 (2000) p.238.

[2] E.I. Samuel, A. Bhowmik, R.S. Qin, J. Mater. Res. 25 (2010) p.1020.

[3] Y. B. Jiang, G.Y. Tang, C. Shek, Y.H. Zhu, Z.H. Xu, Acta Mater. 57 (2009) p.4797.

[4] P. S. Ho, T. Kwok, Rep. Prog. Phys. 52 (1989) p.301.

[5] Y. Dolinsky, T. Elperin, Phys. Rev. B 47 (1993) p.14778.

[6] R.S. Qin, B.L. Zhou, Int. J. Non Equilib. Process. 11 (1998) p.77.

[7] Y. Mohammad, P.C. Sahu, K.G.Rajan, Phys. Rev. B 34 (1986) p.8086.

[8] S.K. Ghosh, S. Mondal, Mater. Charact. 59 (2008) p.1776.

[9] H. Conrad, Mater. Sci. Eng. A 287 (2000) p.227.

[10] V. Randle, Acta Mater. 52 (2004) p.4067.

[11] L. Lu, Y. Shen, X. Chen, L. Qian, K. Lu, Science, 304 (2004) p.422.

[12] X.L. Wang, Y.B. Wang, Y.M. Wang, B.Q. Wang, J.D. Guo, Appl. Phys. Lett. 91 (2007) p.163112.

[13] R.S. Qin, E.I. Samuel, A. Bhowmik. J. Mater. Sci. 46 (2011) p.2838.

[14] R. Badji, M. Bouabdallah, B. Bacroix, C. Kahloun, B. Belkessa, H. Maza, Mater. Charact. 59 (2008) p.447.

[15] K. Ravindranath, S.N. Malhotra, Corros. Sci. 37 (1995) p.121-129, p.131.

[16] I.A. Ibrahim, F.A. Mohamed, E.J. Lavernia, J. Mater. Sci. 26 (1991) p.1137.

[17] K. Shirvani, S. Mastali, A. Rashidghamat, H. Abdollahpour, Corros. Sci. 75 (2013) p.142.